MAGNETIC RESONANCE IN CHEMISTRY
Magn. Reson. Chem. 2004; **42**: 594–599
Published online in Wiley InterScience (www.interscience.wiley.com). DOI: 10.1002/mrc.1399

Heteronuclear selective refocusing 2D NMR experiments for the spectral analysis of enantiomers in chiral oriented solvents

Jonathan Farjon, Jean-Pierre Baltaze, Philippe Lesot, Denis Merlet* and Jacques Courtieu

Laboratoire de Chimie Structurale Organique, UMR CNRS 8074, Université Paris-Sud, ICMMO, Bât. 410, 91405 Orsay Cedex, France

Received 5 January 2004; Revised 16 March 2004; Accepted 19 March 2004

We report the use of carbon–proton heteronuclear selective refocusing 2D NMR experiments dedicated to the spectral analysis of enantiomers dissolved in weakly ordering chiral liquid crystalline solvents. The method permits the extraction of carbon–proton residual dipolar couplings for each enantiomer from a complex or unresolved proton-coupled ^{13}C spectral patterns. Illustrative examples are analysed and discussed. It is shown that an accurate determination of enantiomeric excess is possible. Copyright © 2004 John Wiley & Sons, Ltd.

KEYWORDS: NMR; ^{13}C NMR; chiral liquid crystal; selective pulses; enantiomeric excess

INTRODUCTION

Over the last two decades, selective radiofrequency pulses have been intensively used in liquid-state NMR spectroscopy in order to simplify spectral analysis and to elucidate molecular structures.[1,2] For instance, selective excitations have been used to reduce the dimensionality of multi-dimensional NMR experiments, namely from 3D to 2D and from 2D to 1D. As a direct consequence, the desired spectral information can be obtained faster and with high digital resolution. Selective NMR experiments are also very useful for obtaining specific quantitative spectral data such as the magnitude of scalar couplings or NOE effects.[3–16]

Recently, we have reported an original application of selective NMR excitations applied in the field of chiral analysis. We have shown the practical efficiency of homonuclear selective refocusing 2D experiments (SERF)[17] for the visualization of enantiomers dissolved in weakly ordering chiral liquid crystals based on organic solutions of homopolypeptides such as poly-γ-benzyl-L-glutamate (PBLG).[18,19] This approach has been successfully applied to the determination of enantiomeric purity in enriched mixtures using proton NMR. However, some difficulties may arise for chiral molecules embedded in a chiral liquid crystal when using ^{1}H-SERF. First, the selective refocusing experiments can be applied only if some proton NMR signals are isolated enough to be excited selectively. Second, even if the ability of the chiral polypeptides to discriminate enantiomers is very general,[20] it does not imply necessarily that spectral enantiodiscriminations will be observed through a specific proton–proton dipolar coupling.

*Correspondence to: Denis Merlet, Laboratoire de Chimie Structurale Organique, UMR CNRS 8074, Université Paris-Sud, ICMMO, Bât. 410, 91405 Orsay, France.
E-mail: denismerlet@icmo.u-psud.fr

Chiral discrimination originates in a differential ordering effect of enantiomers inside the chiral oriented phase. Consequently, any order-dependent NMR interactions can be used for visualizing the enantiomers. Indeed, we have already shown that proton–carbon-13 dipolar couplings could provide an excellent alternative when proton NMR fails or gives poor results.[21] However, the sensitivity of the experiment is small and the visualisation of the enantiomers is not trivial in the case of large molecules owing to the numerous long-range dipolar couplings. The present work explores and demonstrates the efficiency of heteronuclear selective refocusing $^{13}C-^{1}H$ NMR experiments, HETSERF, in the analysis of enantiomers dissolved in chiral liquid crystal. In this approach we take advantage of the large chemical shift range of proton decoupled ^{13}C spectra and we reduce the multiplicity of proton coupled ^{13}C lines resulting in an increased sensitivity. We demonstrate that $^{1}H-^{13}C$ selective refocusing 2D experiments provide a valuable NMR tool for analysing a mixture of enantiomers. The efficiency of the method is illustrated on different experimental samples for which the enantiomeric composition was measured.

EXPERIMENTAL

Sample preparation

Liquid-crystalline NMR samples were prepared using a standard procedure.[18] Samples of 1,2-dibromopropane [(±)-DBP] and 2-chloropropanoic acid (*ee* = 26% in the *S* enantiomer) (CPA) were made using 140 and 115 mg of PBLG (MW ≈ 120 000), 80 and 107 mg of enantiomer mixture and 557 and 334 mg of dry $CHCl_3$, respectively. Details of the method and sample preparation can be found in literature.[18] Note that PBLG is commercially available from Sigma and all 5 mm o.d. NMR tubes were sealed to avoid

solvent evaporation and then centrifuged head-to-tail until an optically homogeneous birefringent phase was obtained.

NMR spectroscopy

1D and 2D NMR spectra in oriented solvents were measured at 9.4 T on a high-resolution Bruker Avance 400 MHz spectrometer equipped with a BBO 5 mm probe and a standard variable-temperature unit (BVT 3200). Other experimental details can be found in the figure captions.

Unless specified otherwise, the heteronuclear selective *JD*-resolved 2D experiments were recorded using a data matrix of 2048 (t_2) × 1024 (t_1) with eight scans per t_1 increment for (±)-DBP samples and 4096 (t_2) × 2048 (t_1) with eight scans per t_1 increment for CPA samples. No zero filling and no filtering were used. Signals are phased in both dimensions. A large number of t_1 increment, 1K or 2K, is necessary in order to take advantage of the great narrowing of the lines in the F_1 dimension.

RESULTS AND DISCUSSION

Over 20 years ago, Bax and Freeman[22] developed an efficient 2D NMR method that allows long-range $^1H-^{13}C$ scalar couplings to be measured in isotropic media. The purpose of this sequence was to observe the long-range *J* couplings between a selected proton, or a group of equivalent protons, and all the interacting carbon atoms. It is based on the well-known heteronuclear *J*-resolved 2D experiment but involves a 180° shaped proton r.f. pulse for selecting a single type of proton in the studied molecule. The pulse sequence and the phase cycling are shown in Fig. 1.

The 2D sequence can be briefly described as follows. In the middle of the t_1 ^{13}C evolution period, a 180° REBURP selective pulse is applied on a proton while a 180° hard pulse is applied on carbon-13. These two pulses refocus the ^{13}C chemical shifts and all the carbon–proton couplings except the coupling between the selectively excited proton and all the carbon-13 atoms of the molecule. The amount of information evolving during time t_1 is then reduced to the spin–spin coupling, scalar and dipolar, between the selected proton and the carbons, thus simplifying the analysis of the spectra. Note here that among possible pulse shapes, the REBURP shaped pulse was chosen because it provided the best signal selectivity compared with other tested shaped pulses.[1,23] Another benefit of the sequence is that field inhomogeneities in the sample are refocused during t_1, leading to a narrower linewidth. The sequence ends with the observation of the ^{13}C FID under proton decoupling during t_2. Disregarding all relaxation terms and phase factors and assuming that all phases were set along the *x*-axis of the rotating frame, the expression of the NMR signal, $S(t_1, t_2)$, obtained in a single scan is

$$S(t_1, t_2) = -iA\cos[\pi(J_{CH_i} + 2D_{CH_i})t_1]\exp[i2\pi(\nu_C + \Delta\nu_C)t_2]$$

where A is the amplitude of the signal, ν_C and $\Delta\nu_C$ are the isotropic and anisotropic parts of the carbon resonance frequencies and J_{CH_i} and D_{CH_i} are the scalar and the dipolar couplings between the ^{13}C nuclei and the selected proton spin(s) i, respectively.

A few changes were made compared with the initial work of Bax and Freeman.[22] First, in the original experiment the authors were only interested in the $^1H-^{13}C$ long-range scalar coupling. In our case, the enantiomeric differentiation is often observable on the one-bond dipolar coupling and consequently it is necessary to use a shorter selective pulse to excite the proton ^{13}C satellites. Second, they extracted the lines corresponding to each carbon chemical shift, after Fourier transformation during the acquisition time t_2, to obtain a set of t_1 FIDs. After Fourier transformation on each of these t_1 FIDs, the long-range scalar coupling with proton i were measured. In oriented chiral solvents, this is not suitable because two enantiomers may have different chemical shift anisotropies (CSA). It is then more convenient to achieve a double Fourier transformation. It is also important to carry out a phase-sensitive 2D experiment with pure absorption lineshapes in both dimensions in order to have a better sensitivity and resolution compared with a magnitude 2D map. For this reason, we used the sequential acquisition mode. Then, after a double Fourier transformation, the resulting 2D map shows the spectral pattern associated with the selected $^1H/^{13}C$ pairs in the F_1 dimension while the proton decoupled ^{13}C spectrum appears in the F_2 dimension. The 2D map can be phased but the signal in the F_1 dimension is not in the quadrature mode. This last point is not important as the signal is symmetric with respect to the 0 Hz line in the F_1 dimension.

To demonstrate the ability of this experiment to simplify proton-coupled carbon-13 spectra, we investigated the case of 1,2-dibromopropane in a racemic mixture, (±)-DBP, dissolved in the PBLG–$CHCl_3$ chiral mesophase at 300 K. This example is interesting because the classical 1D proton coupled carbon-13 signal of the methyl group shows a complex unresolved spectral pattern that cannot be interpreted easily, as seen in Fig. 2. This kind of unresolved spectrum is commonly observed when long-range proton–carbon dipolar couplings are numerous. Consequently, it is not possible either to claim unambiguously that the two enantiomers are differentiated in this spectrum, or to measure any precise anisotropic coupling data to obtain further information on the molecular geometry and orientation. Here the use of the heteronuclear selective *JD*-resolved 2D experiments makes such measurements possible.

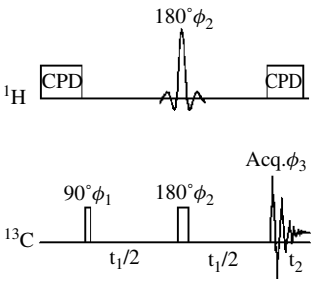

Figure 1. Basic pulse scheme of the 2D experiment. The 16-steps phase cycling is $\phi_1 = \phi_3 = x, -x, x, -x, y, -y, y, -y, -x, x, -x, x, -y, y, -y, y$; $\phi_2 = x, x, -x, -x, y, y, -y, -y, -x, -x, x, x, -y, -y, y, y$. The selective 180° proton pulse is a REBURP shape pulse. The protons are decoupled using the classical WALTZ-16 sequence.

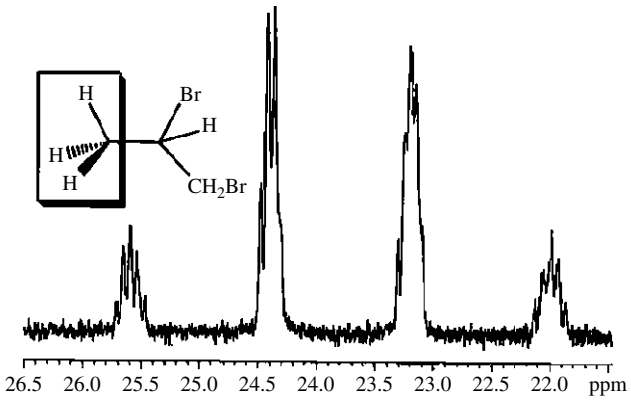

Figure 2. 100.6 MHz proton-coupled carbon spectrum of the methyl group of (±)-1,2-dibromopropane dissolved in the PBLG–$CHCl_3$ phase at 295 K.

Figure 3 shows the heteronuclear selective *JD*-resolved 2D map obtained by selective excitation of the three equivalent methyl protons of (±)-DBP. The proton-decoupled ^{13}C signal is obtained in the F_2 dimension, but here the difference in chemical shift anisotropy is very weak and does not provide separated resonances. In contrast, we clearly observe two quartets in the F_1 dimension for the C_A carbon, from which we can measure easily and precisely the one bond $^{13}C-^1H$ total spin–spin coupling, $|^1T_{CH}| = |^1J_{CH} + 2^1D_{CH}|$, for each enantiomer. In this example, the $|^1T_{CH}|$ values are equal to 123.3 and 118.7 Hz, respectively. Consequently, the evaluation of the enantiomeric composition would be possible in the case of an enantio-enriched sample. Note that

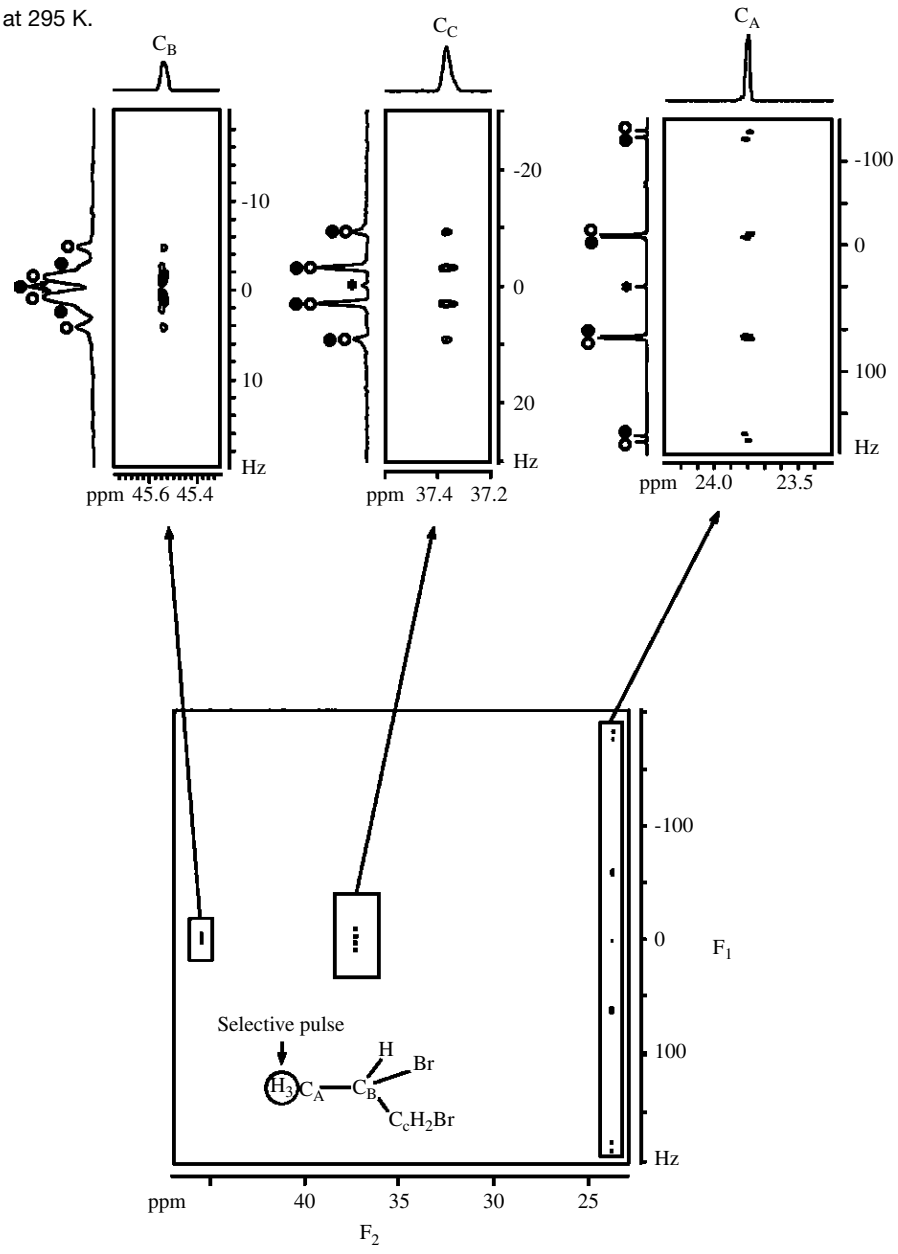

Figure 3. Heteronuclear selective *JD*-resolved 2D spectrum selective on the proton of the methyl group of (±)-1,2-dibromopropane dissolved in the PBLG–$CHCl_3$ mesophase at 300 K. A 14 ms REBURP shaped pulse was applied on the methyl protons (290 Hz selective excitation bandwidth). Enlarged maps of the different carbon signals are shown. The signals belonging to each enantiomers are arbitrarily labelled by open and black circles. The weak artefact at $F_1 = 0$ Hz, marked with an asterisk, is due to pulse imperfections[22].

the relative intensities of the two sub-spectra are equal, as must be the case for a racemic mixture. Note also that the resolution in F_1, $\Delta\nu_{1/2} = 1.5$ Hz, is much better than in the F_2 dimension, $\Delta\nu_{1/2} = 5$–6 Hz and allows the observation in F_2 of a small but measurable CSA of 0.01 ppm, i.e. 1 Hz, that was not observable in the 1D spectrum. The analysis of the other carbon-13 signals of (±)-DBP is also interesting and shows that for the methylenic carbon, C_C, the signal is reduced to a single quartet originating from the total spin–spin coupling with the methyl protons. Here we can measure $|^3T_{CH}| = 6.1$ Hz. Therefore, there is no enantiodiscrimination on this site. This is not the case for the methine carbon, C_B, where two quartets are visible having a splitting of $|^2T_{CH}| = 3.0$ and 1.7 Hz, respectively, for each enantiomer, although a small difference is visible between the enantiomers along this CH direction. In this example, we have shown that the heteronuclear selective *JD*-resolved 2D experiment is a very useful tool which provides analytical information that it is impossible to extract from the standard proton-coupled carbon-13 spectrum.

Having obtained successful experimental results on a racemic mixture, in a second step we investigated the case of an enantiomerically enriched sample. For this purpose, we prepared a 2-chloropropanoic acid (CPA) mixture enriched in the *S*-enantiomer and recorded the heteronuclear selective *JD*-resolved 2D experiments with selective proton pulse on the methyl protons (Fig. 4) and on the methine proton (Fig. 5). As expected for this example, we obtain two separated spectra, one for each enantiomer. Differences in peak intensities quickly reveal the enantiomeric enrichment.

In Fig. 4 we observe two resonances for carbon C_A, separated by 3.0 Hz in the F_2 dimension owing to a difference in ^{13}C CSA, while two quartets with different couplings appear in the F_1 dimension: $|(^1T_{CH})^S| = 137.5$ Hz and $|(^1T_{CH})^R| = 102.7$ Hz. By integrating the signals of each enantiomer on the F_1 projection or on the 3D volume of

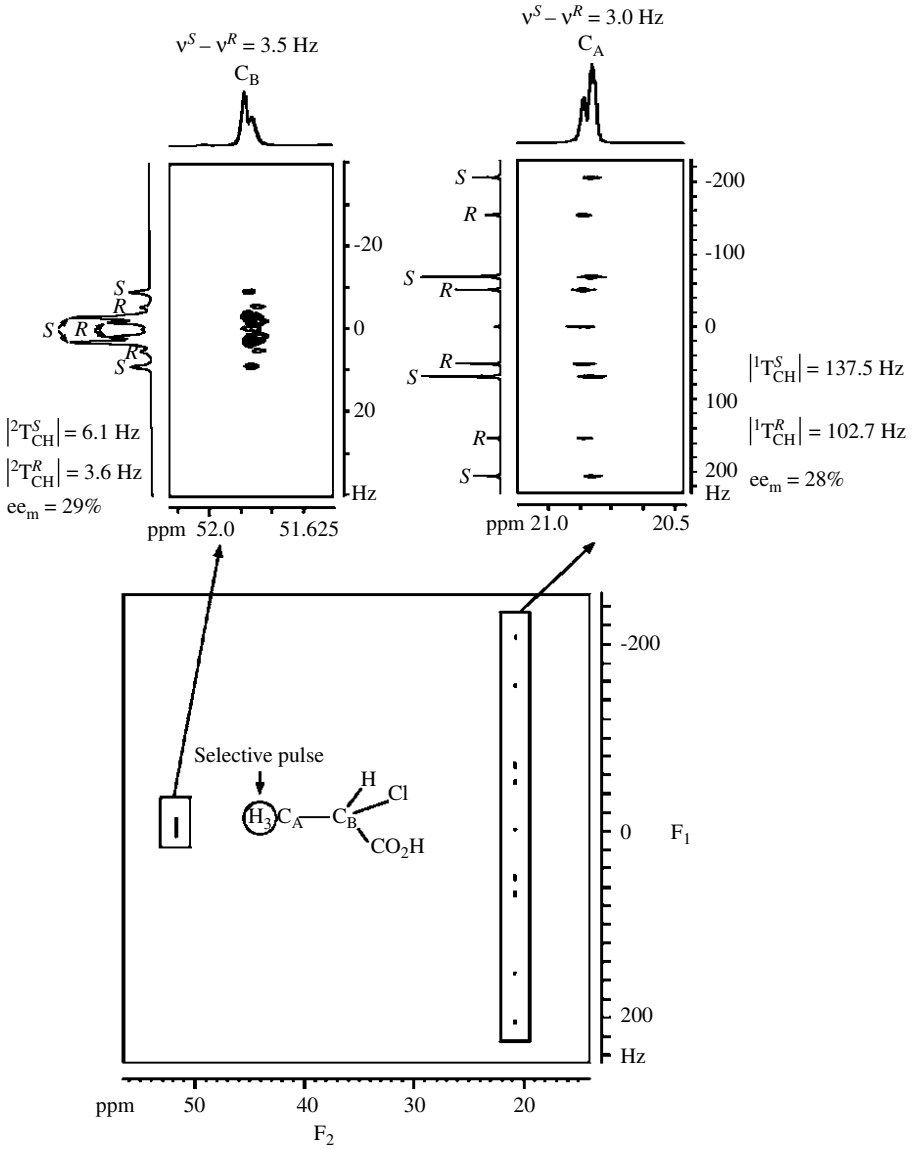

Figure 4. Heteronuclear selective *JD*-resolved 2D spectrum of a *S*-enriched mixture of 2-chloropropionic acid dissolved in the PBLG–$CHCl_3$ phase at 300 K. A 5 ms REBURP 180° selective pulse was applied on the methyl protons (800 Hz selective excitation bandwidth). Enlarged maps show details of the methyl and methine carbon signals. Note the quality of the resolution in F_1.

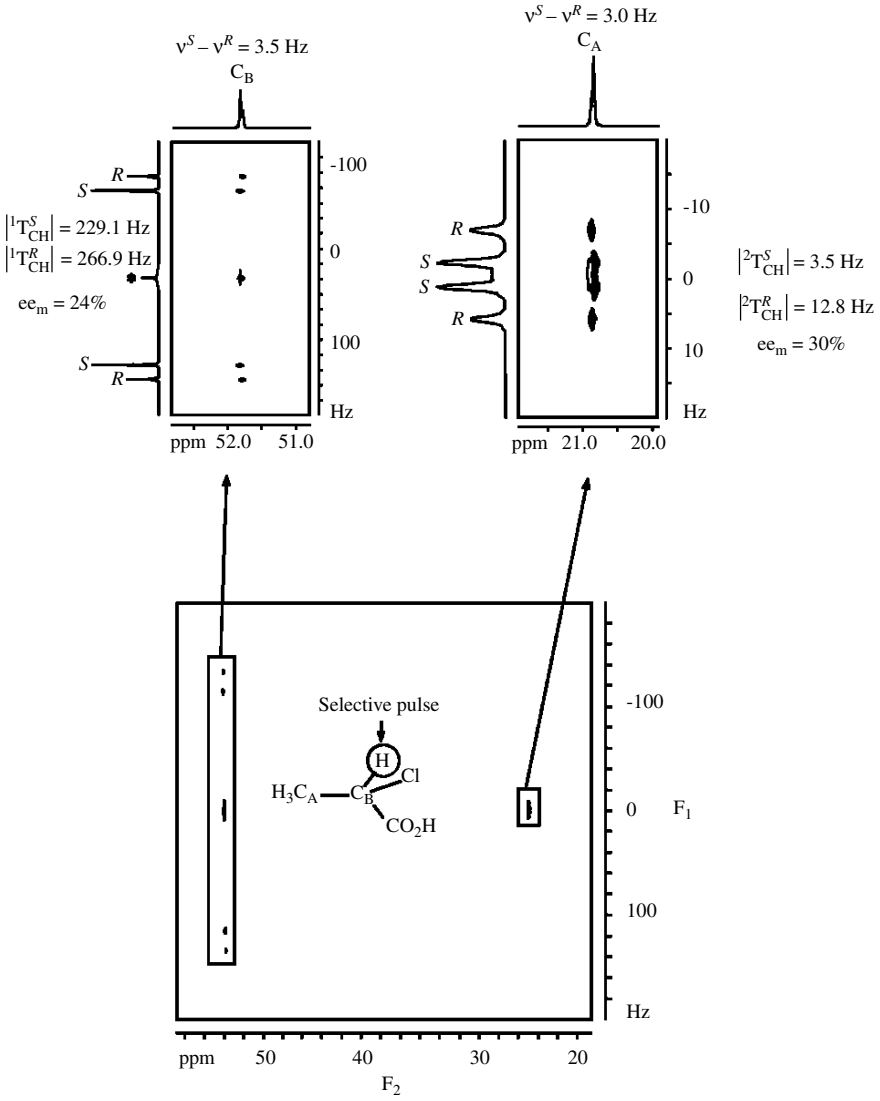

Figure 5. Heteronuclear selective *JD*-resolved 2D map of the *S*-enriched mixture of CPA dissolved in the PBLG–$CHCl_3$ mesophase at 300 K. A 5 ms REBURP 180° selective pulse was applied on the methine proton. Enlarged maps show details on the methyl and methine carbon signals. The weak artefact at $F_1 = 0$ Hz, marked with an asterisk, is due to pulse imperfections[22].

the correlation peaks, we can experimentally evaluate from a series of measurements the enantiomeric excess at 28%. This value is close to the prepared enantiomeric excess of $26 \pm 1\%$ obtained by weighting the mass of each enantiomer. As for carbon C_A, we can see two resonances for carbon C_B, separated by 3.5 Hz in the F_2 dimension owing to a difference in ^{13}C CSA. In the F_1 dimension, carbon C_B exhibits two quartets of different intensities ($|^2T_{CH}|^S = 6.1$ and $|^2T_{CH}|^R = 3.6$ Hz), from which the enantiomeric excess can be calculated as 29% by simple integration of the different signals.

We also used selective pulse on the methine group of the *S*-enriched CPA sample. The 2D map is shown in Fig. 5. For carbon C_A, two weak resolved resonances separated by a CSA difference of 3.0 Hz are observed in the F_2 dimension, one for each enantiomer. The difference in peak intensities reveals already the enantiomeric enrichment but the difference in CSA is not sufficiently large to accurately evaluate the enantiomeric excess. In the F_1 dimension, two doublets centred on zero are obtained, which have also different relative intensities. We can measure the two different long-range total spin–spin couplings associated with the *R* and *S* enantiomers, namely $|(T_{1-4})^R| = 12.8$ Hz and $|(T_{1-4})^S| = 3.5$ Hz. Here again the integration of signals for both enantiomers on the F_1 projection or on the 3D volumes of the correlation peaks in the 2D map is possible and we can evaluate the enantiomeric excess as 30%, which again is close to the prepared value. The spectral pattern observed for the C_B carbon atom is similar to that obtained for C_A, except that the magnitude of the total spin–spin couplings is larger: $|(^1T_{CH})^R| = 266.9$ and $|(^1T_{CH})^S| = 229.1$ Hz. Integrating these signals leads to an enantiomeric excess of 24%, which is close to the real value within 2%. In both Figs 4 and 5, note again the interesting gain in the resolution in the F_1 dimension compared with F_2, by a factor of ~3.

CONCLUSION

Heteronuclear selective *JD*-resolved 2D experiments appear to be an efficient analytical tool, able to simplify considerably

the spectral analysis of proton-coupled carbon spectra of chiral organic compounds dissolved in chiral weakly ordering solvents. This technique noticeably improves the visualization of enantiomeric discrimination by reducing the number of resonances on spectra and by a net gain in the linewidths. Hence it permits the measurement of short- and long-range total spin–spin couplings for each enantiomer. Finally, this method is quantitative and can be used to determine enantiomeric excesses with a fairly good accuracy. Heteronuclear selective *JD*-resolved 2D experiments on large-sized chiral compounds are under way to generalize the approach and evaluate its robustness.

REFERENCES

1. Freeman R. *Prog. Nucl. Magn. Res. Spectrosc.* 1998; **32**: 59.
2. Berger S. *Prog. Nucl. Magn. Res. Spectrosc.* 1997; **30**: 137.
3. Berstein MA, Trimble LA. *Magn. Reson. Chem.* 1994; **32**: 107.
4. Willker W, Leibfritz D. *Magn. Reson Chem.* 1992; **30**: 645.
5. Emsley L, Bodenhausen G. *J. Magn. Reson.* 1989; **82**: 211.
6. Bruschweiler R, Madsen JC, Griesinger C, Sorensen OW, Ernst RR. *J. Magn. Reson.* 1987; **73**: 380.
7. Cavanagh J, Waltho JP, Keeler J. *J. Magn. Reson.* 1987; **74**: 386.
8. Emsley L, Dwyer TJ, Spielmann HP, Wemmer DE. *J. Am Chem. Soc.* 1993; **115**: 7765.
9. Jeannerat D, Bodenhausen G. *J. Magn. Reson.* 1999; **141**: 133.
10. Peng C, Jeannerat D, Bodenhausen G. *Magn. Reson. Chem.* 1997; **35**: 91.
11. Fäcke T, Berger S. *J. Magn. Reson. A.* 1995; **113**: 257.
12. Hurd RE. *J. Magn. Reson* 1990; **87**: 422.
13. Fäcke T, Berger S. *J. Am. Chem. Soc.* 1995; **117**: 9547.
14. Berger S. *Angew. Chem., Int. Ed. Engl.* 1988; **100**: 1198.
15. Wagner R, Berger S. *Fresenius' Z. Anal. Chem.* 1997; **357**: 470.
16. Fäcke T, Berger S. *J. Magn. Reson. A* 1996; **119**: 260.
17. Farjon J, Merlet D, Lesot P, Courtieu J. *J. Magn. Reson.* 2002; **158**: 169.
18. Aroulanda C, Sarfati M, Courtieu J, Lesot P. *Enantiomer* 2001; **6**: 281.
19. Sarfati M, Lesot P, Merlet D, Courtieu J. *Chem. Commun.* 2000; 2069.
20. Lesot P, Sarfati M, Courtieu J. *Chem. Eur. J.* 2003; **9**: 1724.
21. (a) Lesot P, Merlet D, Meddour A, Courtieu J, Loewenstein A. *J. Chem. Soc., Faraday, Trans.* 1995; **91**: 1371; (b) Lesot P, Merlet D, Courtieu J, Emsley JW, Rantala TT, Jokisaari J. *J. Phys. Chem. A* 1997; **101**: 5719.
22. Bax A, Freeman R. *J. Am. Chem. Soc.* 1982; **104**: 1099.
23. Geen H, Freeman R. *J. Magn. Reson.* 1991; **93**: 93.